ELSEVIER

Journal of Crystal Growth 166 (1996) 423–428

JOURNAL OF CRYSTAL GROWTH

Growth of $LiYF_4$ crystals doped with holmium, erbium and thulium

I.M. Ranieri *, S.L. Baldochi, A.M.E. Santo, L. Gomes, L.C. Courrol, L.V.G. Tarelho, W. de Rossi, J.R. Berretta, F.E. Costa, G.E.C. Nogueira, N.U. Wetter, D.M. Zezell, N.D. Vieira, Jr., S.P. Morato

Instituto de Pesquisas Energéticas e Nucleares-CNEN / SP, C.P. 11049, São Paulo, SP-05499-970, Brazil

Abstract

Crystals of $LiYF_4$ (YLF) doped with holmium, erbium, and thulium were successfully grown by the Czochralski technique. The synthesis, growth conditions, and pulsed-laser performance using a $LiY_{0.555}Er_{0.38}Tm_{0.06}Ho_{0.005}F_4$ crystal, are presented.

1. Introduction

Er:Tm:Ho:$LiYF_4$ (YLF) laser emission at 2.065 μm originates from the active holmium ion [1–3]. Erbium and thulium ions act as sensitizers to transfer efficiently the absorbed pumping energy into the holmium metastable-energy state [4]. This system is an eye-safe laser because it is strongly absorbed by water molecules making it suitable for medical applications [5,6]. To produce laser materials, good optical quality and a homogeneous dopant distribution must be achieved in the crystal-growth process.

The optical quality of fluoride crystals depends on the purity of the starting raw materials and the growth conditions [7]. The optical properties of the as-grown crystals are greatly affected by the presence of oxygen complexes. In highly doped rare-earth YLF crystals (RE:YLF), the excitation energy migrates along the ions, and therefore, oxygen traps can efficiently quench this energy [8]. This results in a decrease in the predominant energy transfer to the laser-active holmium ions. The process of obtaining the fluorides from the respective oxides is enhanced by the similarity of the ionic radius of F^- and O^{2-} and due to the higher electronegativity of the F^- ion [9]. It is thus assumed that negligible amounts of O^{2-} are present in the starting materials. Care should be taken then to avoid water vapor contamination in all steps of the crystal-growth process. When oxygen is present, it is usually accompanied by other oxygen complexes, such as ($2F^- = O^{2-} + \square$), domains with fluorine-hydroxyl substitutions [10], $Me(OH)_2$ (Me = Mg, Mn or Ti) complexes [11,12], or HCO^- molecules [13]. These complexes can be easily detected due to their characteristic infrared (IR) absorption spectra around 2.7 μm.

The present work is part of a research program aimed at the development of a medical Ho:YLF laser. High-quality rare-earth-doped YLF crystals were obtained by following a systematic procedure. A reactive atmosphere of gaseous hydrogen fluoride (HF) was used in the synthesis and zone-refining steps of the compound preparation. The crystals were grown by the Czochralski technique in a purified argon atmosphere. A preliminary spectroscopic study of YLF:Er crystals doped with the impurities OH^-

* Corresponding author. Fax: +55 11 212 3546.

SSDI 0022-0248(95)00506-4

and/or Mg^{2+}, as well as the results of laser testing for a $LiY_{0.555}Er_{0.38}Tm_{0.06}Ho_{0.005}F_4$ crystal, are presented.

2. Experimental procedure

2.1. Crystal preparation

ErF_3, TmF_3, HoF_3, and YF_3 were prepared from pure oxide powders (Aldrich and/or Johnson Matthey) with purity of 99.99%. In the synthesis process, the oxides were placed in a platinum boat inside a platinum tube. They were slowly heated in a stream of argon gas (purity of 99.995%) and HF gas (Matheson Products, with a purity of 99.99%) up to 850°C. LiF powder (Aldrich, with purity of 99.99%) was zone-refined before it was added to the YF_3. The YLF was synthesized in the same way with a composition of 49.5% YF_3 and 50.5% LiF, which was the most efficient composition in the zone-refining process. In these experiments, the synthesized YLF was placed in a 300 mm long graphite boat inside a platinum tube. A 20 mm long molten zone was provided by a globar furnace. A single pass was performed along the boat at a transverse rate of 7 mm h^{-1}. Due to the incongruent melting behavior of this material, the characteristic three-zone bar [7] was usually obtained. In general, the stoichiometric YLF phase occupied 90% of the bar. The LiF powder was subjected to four zone-refining passes using a transverse rate of 10 mm h^{-1}.

Single crystals were grown by the Czochralski technique under a purified argon atmosphere using a conventional stainless steel furnace with graphite-resistance heating. The zone-refined YLF and the binary rare-earth fluorides were melted in a platinum crucible after a heat treatment under vacuum. The crystal-pulling rate was 1 mm h^{-1} for [100]-, [001]-, or [110]-oriented boules, and rotation rates were in the range of 20–25 rpm. During the process, the crystal diameter was controlled visually. Small boules weighing up to 50 g and single-doped with Er, Ho, and Tm were grown for spectroscopic studies of the energy-transfer mechanisms. The concentrations were in the range of 1–40 mol% for Er, 1–20 mol% for

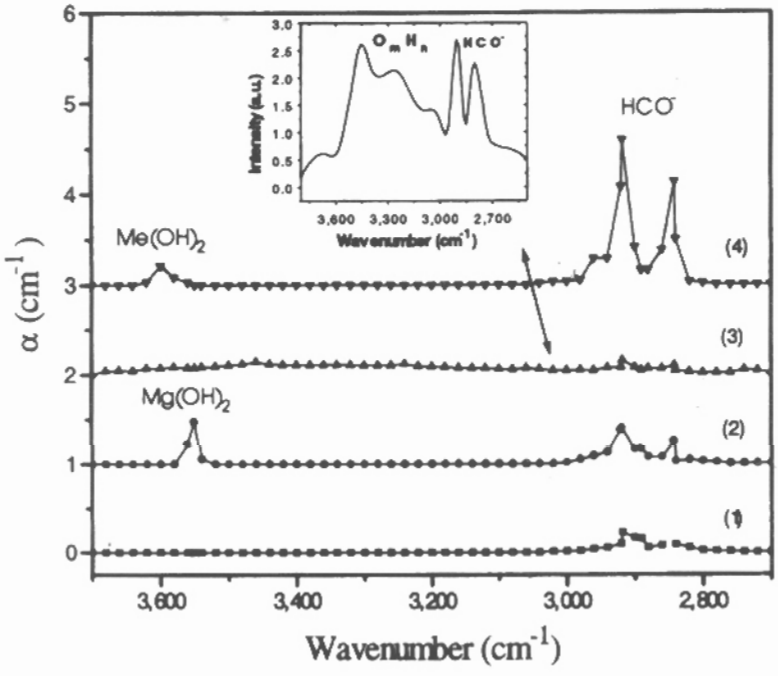

Fig. 1. Absorption spectra of the following crystals: (1) $LiY_{0.555}Er_{0.38}Tm_{0.06}Ho_{0.005}F_4$, (2) Mg^{2+}:OH^-:$LiY_{0.60}Er_{0.40}F_4$, (3) OH^-:$LiY_{0.60}Er_{0.40}F_4$. The insert shows in detail the band shape, and (4) commercial YLF.

Tm, and 0.1–10 mol% for Ho. It was observed that impurities such as OH^- and Me–OH^- complexes can compete with the holmium ions in the energy-transfer processes, leading to a decrease in the excitation efficiency of the laser level [14]. Therefore, two $LiY_{0.60}Er_{0.40}F_4$ crystals were grown for this study, one doped with 0.1 mol% OH^- and another doped with 0.1 mol% OH^- and 1 mol% Mg^{2+} (concentrations in the melt).

Three crystals were grown for the fabrication of laser rods with the following compositions:

$LiY_{0.555}Er_{0.38}Tm_{0.06}Ho_{0.005}F_4$,

$LiY_{0.559}Er_{0.38}Tm_{0.06}Ho_{0.001}F_4$,

and $LiY_{0.53}Er_{0.35}Tm_{0.10}Ho_{0.02}F_4$. The crystals were oriented along the [100] axis and the boules typical dimensions were 30 mm in diameter and 100 mm long. The melt composition was 49% AF_3 ($A = Y^{3+}$, Er^{3+}, Tm^{3+} or Ho^{3+}): 51% LiF in all runs. In most of the growth processes, 80% of the melt was pulled from the crucible.

2.2. Crystal characterization

Some oxygen impurities absorb in the range from 3650 to 2800 cm^{-1}. These particular molecules can compete with the energy-transfer process: $^4I_{13/2}$ (Er) $\rightarrow$ $^5I_7$ (Ho), absorbing the migrating excitation of the $^4I_{11/2}$ and $^4I_{13/2}$ Er^{3+} ions by a quasi-resonant non-radiative transfer [8]. The infrared spectrum in Fig. 1 shows some of these absorption bands. The narrow absorption at 3610 cm^{-1} is attributed to the absorption of $Me(OH)_2$ complexes [11,12]. It is one of a group of narrow absorption bands attributed to these complexes that appear in the range from 3610 to 3550 cm^{-1}. The origin of these bands, however, is not fully understood. The absorptions at 2920 and 2850 cm^{-1} are due to the HCO^- molecule [13]. Curve (1) of Fig. 1 shows the IR spectra of a laser crystal used to produce the rods. There are only traces of HCO^- molecules in marked contrast to a commercial YLF crystal (see curve (4)). The HCO^- complex is due to carbon contamination coming from the oxides, which is not totally eliminated in the synthesis process. This band indicates that there were traces of water vapor during the crystal growth process. No other absorption bands appeared in this range of the YLF transmission spectrum as shown in Fig. 1, therefore, it can be concluded that the starting materials were free of IR-active divalent ions. In curve (2) of Fig. 1, the spectrum of the $LiY_{0.60}Er_{0.40}F_4$ crystal doped with Mg^{2+} and OH^- is shown. Since Mg^{2+} and OH^- where the main dopants, it can be concluded that the absorption at 3550 cm^{-1} is due to the $Mg(OH)_2$ complex in YLF.

The IR spectrum of the $LiY_{0.60}Er_{0.40}F_4$ crystal doped with OH^- is represented by curve (3) in Fig. 1 and by curve (2) in Fig. 2, which shows the absorption spectra of a LiF and a YLF crystal, both doped with OH^- (0.1 mol%) in the melt. In the LiF crystal, the OH^- molecules enter the host lattice as substitutional OH^- defects with an absorption maximum at 3720 cm^{-1}. Otherwise, the OH^- molecules dissociate during the growth of the YLF crystal producing O_mH_n complexes [15] absorbing in a wide spectral range from 4000 to 2400 cm^{-1}. There is no trace of substitutional OH^- defects as observed in LiF crystals. O_mH_n complexes may also act as traps for the $^4I_{11/2}$ and $^4I_{13/2}$ excitation energy of erbium ions when present in highly concentrated YLF crystals. Direct involvement of these molecules in the partial quenching of the $^4I_{13/2}$ level of Er^{3+} ions can strongly interfere with the Ho^{3+} sensitization process in the Er:Tm:Ho:YLF laser crystals.

The dependence of the YLF-crystal optical quality on the concentration of the free divalent ions or carbon impurities, is not yet established. It is, therefore, assumed that, if they are present in the starting

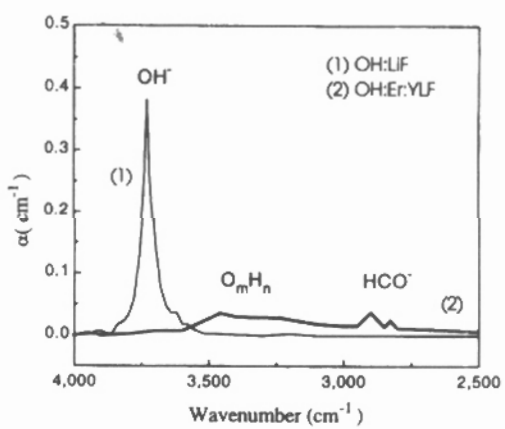

Fig. 2. Absorption spectra of a OH^-:LiF crystal (1) compared with OH^-:$LiY_{0.60}Er_{0.40}F_4$ (2).

materials, the most influential agent is water vapor, since it combines with the impurities thereby originating the IR absorption bands. The $Me(OH)_2$ band has been reported even in YLF crystals grown in an HF atmosphere [16]. The two OH^--doped crystals were visually transparent, but they exhibited a uniform cloudy appearance that scattered light from a focused halogen lamp. This scattering is due to the oxygen-related scattering centers.

The uniformity of the doping distribution along the crystal was inspected by extracting samples from discrete positions along the $LiY_{0.53}Er_{0.35}Tm_{0.10}Ho_{0.02}F_4$ crystal, and the rare-earth concentrations were measured by X-ray fluorescence spectroscopy with an accuracy within 0.5 and 1% (Fig. 3). To determine the effective distribution coefficients of the dopants, the following equation for normal freezing was used:

$$C_S = kC_0(1-g)^{k-1},$$

where C_S is the measured concentration in the samples, C_0 is the initial concentration in the melt, g is the melt solidified fraction, and k is the effective distribution coefficient of each dopant ion. The distribution coefficients were calculated using a least-squares fit, and the following values were obtained: $k_{Ho} = 0.996$ (0.006); $k_{Er} = 1.011$ (0.007); $k_{Tm} = 1.019$ (0.007) and $k_Y = 0.988$ (0.007). The distribution coefficients are very close to 1, as it was expected, due to the similarity of the ionic radii of these heavy rare earths and yttrium. Trace detection techniques, such as high performance liquid chromatography (HPLC) or neutron-activation analysis, would result in more accurate values. Since the YLF is very insoluble, a reliable dissolution method is being developed.

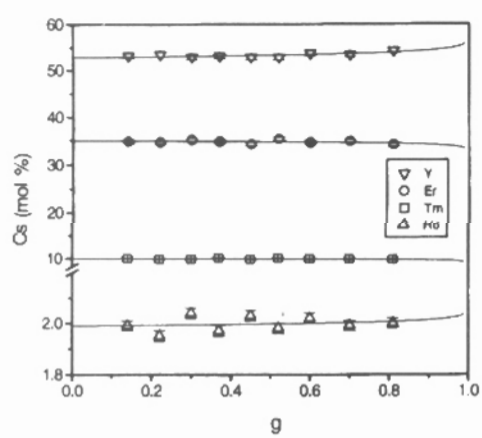

Fig. 3. Distribution of the rare-earth and yttrium ions in the $LiY_{0.53}Er_{0.35}Tm_{0.10}Ho_{0.02}F_4$ crystal.

The growth of heavy rare-earth-doped YLF crystals with uniform doping distribution is facilitated because it is unnecessary to start from large quantities of material in the melt, as required in the case of Nd:YLF, since the neodymium distribution coefficient is much smaller than the unity.

2.3. Laser results

The crystals used to fabricate the laser rods were inspected with a He–Ne laser to detect scattering centers, and they were almost free of scattering centers in the middle of the bulk material. Scattering centers were present in the neck region and in the bottom of the boules due to the sudden changes in the crystal diameter during the crystal-growth process.

Twyman–Green interferometry was used to choose the appropriate regions, and the laser rods were then extracted. Typically, rods with a 5.8 mm diameter and 60–80 mm long were produced. The ends were polished in a special jig to obtain a surface flatness of $\lambda/10$ cm^{-1} at 1 μm, with a parallelism of 30 arcsec.

The best laser results were obtained by using a $LiY_{0.555}Er_{0.38}Tm_{0.06}Ho_{0.005}F_4$ rod. The crystal was pumped by two low-pressure xenon lamps which were located at the foci of a double-ellipse, silver-coated, pumping cavity. The lamps and the rod were water cooled. The laser-rod dimensions were 5.8 mm in diameter and 60 mm long, and the surfaces were not anti-reflection coated. The illuminated length was 45 mm. The resonant cavity had a plano-concave configuration with a long Raleigh parameter, which improves the stability of the laser action in the multi-mode regime. The pump excitation energy was as high as 280 J with a 0.5 Hz repetition rate and a temporal length of 600 μs. Three output mirrors with 65, 75, and 86% reflectivity at 2.065 μm were tested. Fig. 4 shows the output-energy data in relation to the electrical-input energy for laser operation at room temperature. The maximum output power

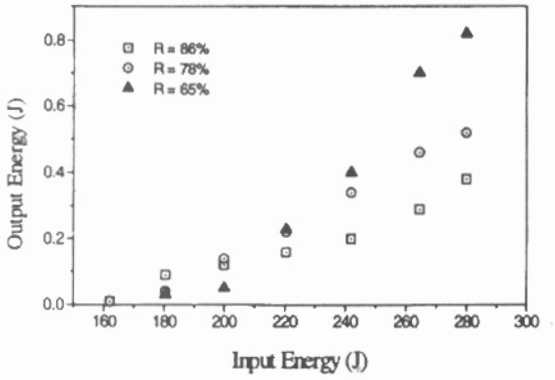

Fig. 4. Laser-output energy as a function of the electrical energy deposited in the flashlamp.

was 820 mJ with a slope efficiency of 0.79% and a threshold in the range of 160 J.

Ho:YLF laser emission originates from the $^5I_7$ electronic manifold and terminates on a Stark component of the $^5I_8$ ground level which has a splitting of 315 cm^{-1}. Thus, it behaves as a quasi-three-level system at room temperature. Therefore, cooling of the rod is necessary in order to enhance the output power. The rod temperature was decreased from room temperature down to 5°C, by coupling the water-cooling system to a heat-exchanger. Fig. 5 shows the increase in the output energy up to a maximum of 1.7 J/pulse. The laser operated with a 65% reflectivity output mirror and 280 J of pumping energy. The laser performance of the $LiY_{0.555}Er_{0.38}Tm_{0.06}Ho_{0.005}F_4$ rod is good compared to that reported in Ref. [3]. The output energies obtained are suitable for dental applications such as etching of dental enamel and the treatment of dental cavities [17].

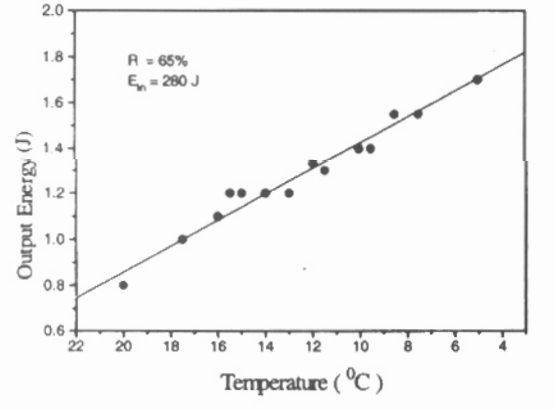

Fig. 5. Laser-output energy as a function of the laser-rod temperature.

3. Conclusion

By following a systematic procedure for the synthesis and growth of YLF crystals, it is possible to obtain relatively pure crystals, as traces of water vapor can be detrimental to laser action in these crystals, The absorption at 3550 cm^{-1} was identified as a main absorption band from the $Mg(OH)_2$ complex absorption band in OH^-:Mg^{2+}:YLF crystals. The performance of the $LiY_{0.555}Er_{0.38}Tm_{0.06}Ho_{0.005}F_4$ crystal as a laser-active medium resulted in a maximum output energy value of 1.7 J/pulse at 5°C, making it suitable for dental applications.

Acknowledgements

We are grateful to FINEP-PADCT which supported this work. I.M.R., L.C.C., L.V.G.T., F.E.C., D.M.Z., and N.U.W. thank FAPESP, CNPq, and RHAE for financial support. The authors are indebted to V.L. Salvador for the X-ray fluorescence analysis.

References

[1] R.L. Remski, L.T. James, Jr., K.H. Goohen, B. Di Bartolo and A. Linz, IEEE J. Quantum Electron. QE 5 (1969) 214.
[2] E.P. Chiclis, C.S. Naiman, R.C. Folweiler, D.R. Gabbe, H.P. Jensen and A. Linz, Appl. Phys. Lett. 19 (1971) 119.
[3] Y. Kalisky, J. Kagan, D. Sagie, A. Brenier, C. Pedrini and G. Boulon, J. Appl. Phys. 70 (1991) 4095.
[4] E.P. Chiclis, C.S. Naiman, R.C. Folweiler and J.C. Doherty, IEEE J. Quantum Electron. QE 8 (1972) 225.
[5] K.T. Thompson, Q.S. Ren and J.-M. Parel, Proc. IEEE 80 (1992) 838.
[6] D.M. Zezell, S.C.M. Cecchini, C.P. Eduardo, K. Matsumoto, W. de Rossi, G.E.C. Nogueira, J.R. Berretta, N.D. Vieira, Jr. and S.P. Morato, J. Clin. Lasers Med. Surg. 13 (1995) 283.
[7] B. Cockayne, J.G. Plant and R.A. Clay, J. Crystal Growth 54 (1981) 407.

[8] M.B. Camargo, L. Gomes and S.P. Morato, Opt. Mater. 4 (1995) 597.
[9] P. Hagenmuller, General Trends in Inorganic Solid Fluorides – Chemistry and Physics, Mater. Sci. Technol. Ser., Ed. P. Hagenmuller (Academic Press, New York, 1985) ch. 1.
[10] A. Macbeuf, G. Demazeau, S. Turrel and P. Hagenmuller, J. Solid State Chem. 3 (1971) 677.
[11] K. Guckelsberger, J. Phys. Chem. Solids 41 (1980) 1209.
[12] S.P. Morato, L.C. Courrol, L. Gomes, V. Kalinov and A. Shadarevich, Phys. Status Solidi (b) 163 (1991) K61.
[13] D.A. Dixon, A. Komornicki and W.P. Kraemes, J. Chem. Phys. 81 (1984) 3603.
[14] L.C. Courrol, L. Gomes and S.P. Morato, Phys. Rev. B 51 (1995) 3344.
[15] Z.G. Akvlediani, K.-J. Berg and G. Berg, Cryst. Lattice Defects 8 (1980) 167.
[16] R. Uhrin, R.F. Belt and V. Rosati, J. Crystal Growth 38 (1977) 38.
[17] C.P. Eduardo, D.M. Zezzell, S.C.M. Cecchini, W. de Rossi, I.M. Ranieri, S.P. Morato and K. Matsumoto, in: Proc. 4th Int. Cong. on Lasers in Dentistry, Singapore (1994).